Vectorlike dark matter within an alternative left-right symmetric model

Yassine Bouzeraib[*]
LPTh, Department of Physics, Faculty of Exact and Computer Sciences, University of Jijel, B. P. 98 Ouled Aissa, 18000 Jijel, Algeria

Mohamed Sadek Zidi[†]
LPTh, Department of Physics, Faculty of Exact and Computer Sciences, University of Jijel, B. P. 98 Ouled Aissa, 18000 Jijel, Algeria

Geneviève Bélanger[‡]
Laboratoire d'Annecy de Physique Théorique, CNRS-USMB, 74940 Annecy, France

(Received 11 March 2026; accepted 24 April 2026; published 26 May 2026)

We investigate an extension of the left-right symmetric model featuring an additional non-Abelian $SU(2)$ gauge symmetry. The particle content is augmented by one generation of vectorlike leptons transforming under the fundamental representation of this new gauge group. We demonstrate that the neutral component of the vectorlike lepton multiplet naturally provides a viable and stable dark matter candidate. Stability is ensured by imposing a discrete parity symmetry that forbids mixing between the vectorlike leptons and the Standard Model leptons. As a consequence, the dark sector interacts with the visible sector exclusively through the vector portal (via s-channel processes) and the vectorlike lepton portal (via t-channel processes). In our analysis, we incorporate collider constraints on the mass of the first-generation extra charged gauge boson $W'^{\pm}$, while assuming that additional scalar states are decoupled from the relevant energy scale for simplicity. We identify the regions of parameter space consistent with the observed relic abundance, collider bounds on the charged partner $E^{\pm}$, current direct detection limits from the LUX-ZEPLIN experiment and indirect detection constraints from Fermi-Large Area Telescope. We find viable dark matter with a mass at the TeV scale. We show the complementarity of direct and indirect searches in probing the remaining parameter space of the model, in particular comparing the prospects of multiton direct detection experiments such as Xenon-Lux-Zeplin-Darwin and of the Cherenkov Telescope Array.

DOI: 10.1103/ksx2-z8s3

I. INTRODUCTION

The left-right symmetric model (LRSM) [1–7] is a well-known extension of the Standard Model (SM) that has been developed over several decades, primarily to account for parity violation in weak interactions and to provide an explanation for neutrino masses through the seesaw mechanism [8,9]. Despite its theoretical appeal, the LRSM does not automatically provide a viable dark matter (DM) candidate. It is therefore natural to investigate whether the framework can be extended to address the dark matter problem.

Many attempts have been made to incorporate a DM candidate within the LRSM framework. One possibility consists in lowering the mass of a right-handed neutrino (RHN) to the keV scale, thereby rendering it a long-lived warm DM candidate [10]. Alternatively, by imposing a discrete Z_2 symmetry on the scalar triplets –under which the left triplet Δ_L is odd and the right triplet Δ_R is even– and setting the vacuum expectation value (VEV) of Δ_L to zero, the neutral component Δ_L^0 becomes a viable DM candidate [11]. Unfortunately, the first approach is rather unnatural within the LRSM framework, while in the second approach Δ_L^0 cannot reproduce the observed relic density due to its small annihilation cross section [12].

These limitations have motivated various extensions of the LRSM to address the DM problem. For example, the LRSM can be extended by adding a scalar singlet [13] or a fermionic singlet [14] that plays the role of DM. Other possibilities include left-right fermion triplets and quintuplets forming a viable two-component DM scenario [11].

[*]Contact author: yassine.bouzeraib@univ-jijel.dz
[†]Contact author: mohamed.sadek.zidi@univ-jijel.dz
[‡]Contact author: genevieve.belanger@lapth.cnrs.fr

Published by the American Physical Society under the terms of the Creative Commons Attribution 4.0 International license. Further distribution of this work must maintain attribution to the author(s) and the published article's title, journal citation, and DOI. Funded by SCOAP³.

Additional proposals involve stable fermionic or scalar multiplets whose stability is ensured purely by the gauge structure, without the need for an *ad hoc* stabilizing symmetry [15], or models in which the gauge group is extended to $SU(3)_C \times SU(2)_L \times U(1)_L \times SU(2)_R \times U(1)_R$ [16] containing a scalar bidoublet and a singlet fermionic DM candidate. Models in which DM arises as a mixture of two or more multiplets have also been studied [17], as well as scenarios where the fermion sector is extended by an additional heavy right-handed copy, with the lightest heavy neutrino acting as DM [18]. Another possibility, which we explore in this work, is to extend the LRSM by introducing vectorlike leptons (VLLs) [19].

In this paper, we extend the gauge structure of the LRSM by introducing an additional $SU(2)$ gauge symmetry, under which one generation of VLF doublets are charged. The model, first introduced in Ref. [20], aims to address several open questions, including the origin of parity violation, neutrino mass generation, and the nature of dark matter. Here, we are primary interested in the possibility that the vectorlike neutrino (N) could serve as a DM candidate. To ensure cosmological stability of N, we assume the existence of a new symmetry in the dark sector. However, imposing a discrete Z_2 symmetry—commonly invoked in the literature to stabilize DM—is not viable in this scenario due to the structure of the Yukawa interactions between the VLFs, the chiral fermions, and the scalar sector. To overcome this issue, we introduce a new parity symmetry that forbids mixing between the VLLs and the chiral leptons [19]. As a consequence, the dark sector particles interact exclusively through the vector bosons portal or through the VLLs portal. The dark sector consists of the VLLs, namely the DM candidate N and its charged partner $E^{\pm}$. For simplicity, we assume that the scalar sector is very heavy and effectively decoupled from the energy scale of interest. Moreover, we neglect the presence of vectorlike quarks (VLQs), as their inclusion does not significantly affect the constraints on the extra gauge bosons derived in Ref. [20]. The most stringent bounds arise from gauge boson decays into the second generation of heavy neutrinos (HNs), which are unaffected by the presence of VLQs.

As in other models where RHNs couple to new gauge bosons [21], the DM relic density falls within the narrow range measured by *Planck* [22] when the total mass of the initial particles in the annihilation (or coannihilation) processes is close to the mass of the mediator, namely one of the neutral or charged gauge bosons of the model. Our goal in this paper is to assess the viability of this LRSM extension in light of current dark matter constraints. After imposing collider limits on the new gauge bosons [20], we require that the predicted relic density does not exceed the upper bound determined by *Planck* observations. Additional constraints from Large Electron Positron Collider (LEP) and LHC searches for new fermions, together with recent limits from direct detection (DD) experiments such as LUX-ZEPLIN (LZ) [23], push the DM mass above the TeV scale. We also consider limits from dark matter indirect detection (ID) searches for γ rays from dwarf spheroidal galaxies by the Fermi Large Area Telescope (Fermi-LAT) [24,25]. However, these mainly constrain the low-mass region, which is already excluded by collider and cosmological bounds.

Finally, we evaluate the prospects for probing this model in future experiments. In particular, we consider projected sensitivities from next-generation liquid xenon direct detection experiments such as Xenon-Lux-Zeplin-Darwin (XLZD)/Dark Matter Wimp Search with Liquid Xenon (DARWIN) [26], and from indirect detection experiments such as Cherenkov Telescope Array (CTA) [27], which are especially relevant for TeV-scale dark matter.

The paper is organized as follows: the model is briefly reviewed in Sec. II. Section III focuses on properties of the dark sector. Section IV includes constraints on the gauge bosons masses as well as other collider constraints. Section V includes a discussion of the dark matter observables for a few benchmarks, while the results of a general scan of the model defining the currently allowed parameter space as well as future probes is performed in Sec. VI. Section VII contains our conclusions.

II. THE MODEL

We consider an extension of the LRSM which includes one generation of vectorlike leptons. The VLLs belong to doublets of an extra gauge symmetry $SU(2)_V$. The vectorlike nature of the VLLs requires that both their chiral components belong to the same representation (the fundamental in this case). Consequently, their masses can be included directly in the Lagrangian without spoiling gauge invariance. The left and right chiral components of SM fermions belong to doublets under the fundamental representations of $SU(2)_L$ and $SU(2)_R$, respectively, as invoked in the LRSM. Under the $SU(2)_V \times SU(2)_L \times SU(2)_R \times U(1)_{B-L}$ gauge group, the VLLs transform as

$$L_{L,R} = \begin{pmatrix} N \\ E \end{pmatrix}_{L,R} \sim (2,1,1)_{-1}, \tag{1}$$

where the subscript "-1" denotes the $B-L$ quantum number.

The gauge bosons fields and the gauge couplings of the model are denoted by

$$\begin{aligned} &SU(2)_V:\ W_V^i, g_V \qquad SU(2)_L:\ W_L^i, g_L \\ &SU(2)_R:\ W_R^i, g_R \qquad U(1)_{B-L}: B, g', \end{aligned} \tag{2}$$

where $i = 1, 2, 3$ is the index of the gauge bosons components.[1] The left-right symmetry imposes the

[1]In the mass basis, the gauge bosons include those of the standard model $\gamma, W^{\pm}, Z$, as well as four heavier gauge bosons $W'^{\pm}, Z', W''^{\pm}$, and Z''.

following conditions on the left- and right-handed parts of the fermionic and gauge fields:

$$\Psi_L \leftrightarrow \Psi_R \qquad \vec{W}_{L\mu} \leftrightarrow \vec{W}_{R\mu}, \tag{3}$$

which leads to

$$g_L = g_R = g, \tag{4}$$

where g is the SM weak coupling.

The scalar sector of the model contains a bidoublet field Φ and left (right) triplets Δ_L (Δ_R), which are introduced to spontaneously break the left/right symmetry of the model. These fields generate the chiral fermions interaction in the Yukawa sector and provide Majorana mass term for the neutrinos. To break the $SU(2)_V$ symmetry and allow the VLLs to mix with the chiral leptons, we need to introduce the two following self-dual bidoublet scalar fields:

$$\Phi_{VL} = \begin{pmatrix} \phi_1^0 & -\phi_1^+ \\ \phi_1^- & \phi_1^{0*} \end{pmatrix} \sim (2,2,1)_0,$$
$$\Phi_{VR} = \begin{pmatrix} \phi_2^0 & -\phi_2^+ \\ \phi_2^- & \phi_2^{0*} \end{pmatrix} \sim (2,1,2)_0. \tag{5}$$

We recall that the VEVs of Δ_R and Φ_{VR} can be taken to be zero as shown in Ref. [20]. The pattern of the symmetry breaking of the model is schematized as follows:

$$SU(2)_V \times SU(2)_L \times SU(2)_R \times U(1)_{B-L} \xrightarrow[\langle\Phi_{VL}\rangle=0]{\langle\Phi_{VR}\rangle=u_R}$$
$$SU(2)_L \times SU(2)_R \times U(1)_{B-L} \xrightarrow[\langle\Delta_L\rangle=0]{\langle\Delta_R\rangle=v_R}$$
$$SU(2)_L \times U(1)_Y \xrightarrow{\langle\Phi\rangle=\mathrm{diag}(k_1,k_2)} U(1)_{EM}, \tag{6}$$

where the VEVs u_R and v_R are both at the TeV scale, and $k_1^2 + k_2^2 = v_{EW}^2$, where v_{EW} is the SM VEV. The bidoublet Φ VEVs can be parametrized as follows:

$$k_1 = v_{EW} c_\beta \qquad k_2 = v_{EW} s_\beta. \tag{7}$$

We assume $k_2 \ll k_1$, following Ref. [28].[2] Thus, the angle β is small [i.e., $\sin(\beta) = s_\beta \sim 0$ and $\cos(\beta) = c_\beta \sim 1$]. The symmetry breaking hierarchy ($u_R > v_R$) imposes that the masses of the second-generation extra-gauge bosons (W'' and Z'') be larger than those of the first-generation (W' and Z'). At first order in ϵ_1 and ϵ_2, with

$$\epsilon_1 = v_{EW}^2/u_R^2 \ll 1 \qquad \epsilon_2 = v_{EW}^2/v_R^2 \ll 1, \tag{8}$$

the gauge bosons mass squared are given by (cf. Ref. [20]):

$$m_W^2 \simeq \frac{1}{4} g^2 v_{EW}^2$$
$$m_{W'}^2 \simeq \frac{g^2 g_V^2}{4(g^2+g_V^2)}(v_{EW}^2 + 2v_R^2)$$
$$m_{W''}^2 \simeq \frac{1}{4(g^2+g_V^2)}(2(g^2+g_V^2)^2 u_R^2 + g^4(v_{EW}^2 + 2v_R^2))$$
$$m_Z^2 \simeq \frac{1}{4} g^2 \frac{v_{EW}^2}{c_W^2}$$
$$m_{Z'}^2 \simeq \frac{1}{4}\left(-\frac{e^2}{c_W^2} + \frac{g^2 g_V^2}{g^2+g_V^2}\right) v_{EW}^2 - \frac{c_W^2 g^4 g_V^4}{(g^2+g_V^2)(e^2 g^2 + (e^2 - c_W^2 g^2) g_V^2)} v_R^2$$
$$m_{Z''}^2 \simeq \frac{1}{4(g^2+g_V^2)}(2(g^2+g_V^2)^2 u_R^2 + g^4(v_{EW}^2 + 4v_R^2)), \tag{9}$$

where c_W and e are the cosine of the Weinberg angle and the electromagnetic coupling, respectively. We recall that the gauge couplings are related by

$$g_L = g_R = g = \frac{e}{s_W} \qquad g' = \frac{g g_V s_W}{\sqrt{c_W^2 g_V^2 - s_W^2(g^2+g_V^2)}}. \tag{10}$$

The gauge coupling g_V is a free parameter, constrained from above using the perturbative unitarity condition $g_V < \sqrt{4\pi}$. It is also bounded from below by requiring that g' in Eq. (10) be real, therefore,

$$g_V > \frac{2\sqrt{\pi} s_W g}{\sqrt{4\pi(c_W^2 - s_W^2) - s_W^2 g^2}}. \tag{11}$$

We emphasize that the last relation ensures that both g' is real and the perturbative unitarity condition is satisfied.

The mixing of the VLLs with the chiral leptons is achieved through the self-dual bidoublet scalar fields. Thus, the Yukawa Lagrangian describing this mixing is given by

$$\mathcal{L}_{\mathrm{int}} = -\bar{L}_R \lambda_l^\dagger \Phi_{VL} l_L - \bar{L}_L \lambda_l' \Phi_{VR} l_R + \mathrm{H.c.}, \tag{12}$$

where λ_l and λ_l' are 3×1 (1×3) Yukawa coupling matrices.

The scenario where N plays the role of DM requires that it must be stable on cosmological times scales. This stability strongly suggests the existence of a new symmetry in the dark sector. There are many possibilities for symmetries that stabilize DM; for example, the discrete Z_2 symmetry which is commonly used [29–39]. Obviously, this possibility cannot be used in our case because this symmetry imposes that both the VLLs and the self-dual bidoublets must be odd fields [i.e., $L_{L,R} \to -L_{L,R}$, $\Phi_{VL(R)} \to -\Phi_{VL(R)}$] under Z_2, while all other fields should be even. Φ_{VL} could be an odd field when the VEV is zero, $\langle\Phi_{VL}\rangle = 0$. In contrast, the

[2]To ensure the known mass hierarchy for the ordinary top and bottom quarks, we must take $k_2 \ll k_1$; see Ref. [28] for more details.

VEV of Φ_{VR} should be at TeV scale; hence, it could not be an odd field under Z_2. To circumvent this problem, one can include a new parity symmetry which disallows mixing between the VLLs and the ordinary leptons [19]; under this symmetry, only the VLLs are odd fields while all other fields are even, such that $\lambda_l = \lambda_l' = 0$. The latter symmetry implies independent free masses for the vectorlike neutrino N and the charged partner $E^{\pm}$. As will be seen in the following sections, their masses will be constrained by phenomenological requirements, mainly by imposing the DM relic density constraint as well as the constraints from the DD and ID approaches. In this scenario, neutrinos get their masses through the seesaw mechanism as invoked, usually within the LRSM, since there is no mixing with the VLL [4,5,8,9].

In the following sections, we will examine various experimental constraints on the relevant parameter space for the DM study; for this, it is more convenient to use the physical parameters as free parameters. The free parameters include the coupling g_V, the VEV of $\langle \Phi_{VR} \rangle$ (u_R), as well as the mass of one extra gauge boson, $m_{W'}$. In the following, we fix $u_R = v_R + 100$ GeV, thus the masses of new gauge bosons can all be rewritten in terms of g_V and $m_{W'}$. This choice is based on the pattern of symmetry breaking followed in Eq. (6), which ensures that both VEVs are at the TeV scale and that u_R is larger than v_R, but not excessively so. This choice is convenient because it guarantees that the first-generation extra gauge bosons W' and Z' are lighter than the second-generation ones W'' and Z'', while the latter remain accessible at colliders and contribute to dark matter physics. In addition, we fix the mass of the HNs to be $m_{W'}/2$ since this relation is used to obtain the collider limits on the heavy gauge bosons. Moreover, with this assumption, the mass of the heavy neutrinos should be at the TeV scale as expected in the seesaw mechanism for neutrino masses. We keep the same feature for the rest of the analysis. For the sake of simplicity, all the masses of the extra scalar bosons are considered to decouple from the scale of interest. Finally, in the dark sector, the two parameters relevant for computing DM observables are the mass of the DM candidate m_N and its mass splitting with the charged partner $E^{\pm}$ which is denoted by Δ_m.

III. DARK SECTOR INTERACTIONS

In the following, we discuss the interactions among the dark sector particles and their relevance for DM annihilation and coannihilation processes. There are two types of channels for which the annihilation and the coannihilation of dark particles can proceed: first, the s-channel processes mediated exclusively by the vector bosons (see the upper diagrams of Fig. 1), and second, the t-channel annihilation processes into vector bosons mediated by the VLLs of the dark sector (see the lower diagrams of Fig. 1). Technically, any combination of particles that interact with one of the gauge bosons (i.e., the fermions,[3] the gauge bosons,[4] and the Higgs boson[5]) could be present in the final states of the s-channel processes provided they are kinematically allowed. On the other hand, the final sates for the t-channel can be exclusively the gauge bosons. This is a consequence of the symmetry imposed for stabilizing the DM particle which disallows interactions of the VLLs through Yukawa couplings.

Although any combinations of the gauge bosons that satisfy the conservation of electric charge can be produced in the final state for the coannihilation processes, in our model, the $Z''/W''^{\pm}$ are kinematically forbidden. Moreover, one should mention that there is no interaction between the DM particle and the photon (i.e., in middle lower diagram of Fig. 1). All possible final states for the s-channel diagrams (i.e., the upper diagrams of Fig. 1) are listed here:

$$
\begin{aligned}
N\bar{N}(E^+E^-) \to V^0 \to &\begin{cases} q\bar{q}, l_i^+ l_i^- \\ \nu_i\nu_i, \nu_i N_i, N_i N_i \\ W^+W^-, W^{\pm}W'^{\mp} \\ Zh, Z'h \end{cases} \\
N(\bar{N})E^{\pm} \to V^{\pm} \to &\begin{cases} q\bar{q}' \\ \nu_i l_i^{\pm}, N_i l_i^{\pm} \\ \gamma W^{\pm} \\ ZW^{\pm}, ZW'^{\pm}, Z'W^{\pm} \\ W^{\pm}h, W'^{\pm}h \end{cases} \\
&\begin{cases} N\bar{N}(E^+E^-) \to Z/Z' \to W'^{\pm}W'^{\mp} \\ N(\bar{N})E^{\pm} \to W^{\pm}/W'^{\pm} \to \gamma W'^{\pm}, Z'W'^{\pm} \end{cases} \\
E^+E^- \to \gamma \to &\begin{cases} q\bar{q}, l_i^+ l_i^- \\ W^+W^-, W'^{\pm}W'^{\mp} \\ W^{\pm}W'^{\mp}, \end{cases}
\end{aligned}
\tag{13}
$$

where q represent the quarks and i the generation index for the leptons [charged leptons ($l_i^{\pm}$), Majorana neutrinos (ν_i), and HNs (N_i)], and $V^0(V^{\pm})$ stands for the neutral (charged) gauge bosons.

The couplings for the interaction of the VLLs with the gauge bosons are summarized in Table I. They depend on the angles used for the diagonalization of the mass matrices of the gauge sector in Ref. [20], namely:

$$
c_1 = \frac{g_V}{\sqrt{g^2 + g_V^2}} \qquad c_2 = \frac{g g_V}{\sqrt{g'^2(g^2 + g_V^2) + g^2 g_V^2}}. \tag{14}
$$

[3]Including the SM fermions (f) and the heavy neutrinos.

[4]Including the photon γ, the neutral gauge bosons $V^0 = Z, Z', Z''$ and the charged gauge bosons $V^{\pm} = W^{\pm}, W'^{\pm}$, and $W''^{\pm}$.

[5]Since the scalar sector is decoupled from the energy scale of interest for the sake of simplicity, the Higgs boson (h) is the only scalar that could appear in the final state.

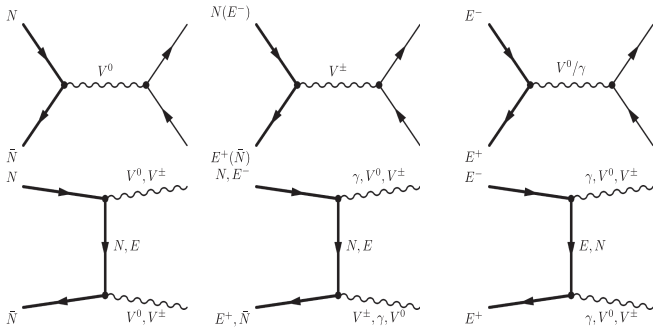

FIG. 1. Feynman diagrams for the annihilation and coannihilation processes via the vector boson/vectorlike lepton portals. In addition to fermions in the final state, the s-channel processes (upper diagrams) can involve gauge bosons and/or the Higgs; see Eq. (13).

Clearly, the interactions via Z and $W^\pm$ are suppressed since they are proportional to the suppressed parameters $\epsilon_{1,2}$ and s_β defined in Eq. (8). Moreover, the $N\bar{N}Z$ coupling is very strongly suppressed because of the multiple powers of small mixing angles entering its definition. This interaction do not contribute significantly to the dark matter formation, as we will see. Thus, the efficient annihilation can be realized exclusively via Z' and Z''. On the other hand, efficient coannihilation can proceed via the three charged gauge bosons ($V^\pm$), although the interaction with $W^\pm$ is somewhat suppressed in comparison with the others.

IV. COLLIDERS CONSTRAINTS

A. LHC constraints on the bosons masses

Current constraints from the LHC on new heavy gauge bosons were derived in Ref. [20], and Table I shows the experimental limits on $m_{W'}$ (consequently $m_{Z'}$). The most restricting limits arise from the $N_2\mu^\pm$ channel [i.e., $pp \to W'^\pm \to N_2\mu^\pm(N_2 \to \mu^\pm q\bar{q}\,')$]. These results could be exploited for getting an indirect lower limit on the second-generation extra-gauge bosons ($W''^\pm$ and Z'') masses. Since the pattern of symmetry breaking is chosen such that $(u_R > v_R)$, we obtain the following mass hierarchies $(m_{W''}$ and $m_{Z''}) > (m_{W'}$ and $m_{Z'})$. Moreover by fixing $u_R = v_R + 100$ GeV for covering as many as possible benchmark points during the analysis, one is able to derive a lower bound on all the gauge boson masses from the experimental lower limit on $m_{W'}$. The results are represented in Table II.

The results in this table were derived for a benchmark point where the mass of the three generations of the HNs are $m_{N_i} = m_{W'}/2$, thus we will keep this assumption for the rest of the analysis. Furthermore, all the masses of the extra bosons from the scalar sector were fixed at a scale of several tens of TeVs.

B. LEP constraints on $E^\pm$ mass

Two types of constraints from LEP on charged leptons are relevant. First, the precise measurement of the Z boson partial decay width at LEP 1, $\Gamma(Z \to E^-E^+) < 2$ MeV [41] rules out the region where the Z boson could decay into E^-E^+, that is, when $m_E < m_Z/2$. Second, when $m_Z/2 < m_E \lesssim 104$ GeV, reinterpreting the LEP 2 [42] limits on chargino mass allow us to exclude all the points in this region. We can apply directly these results because the production cross section is dominated by γ exchange which is a model-independent process. We apply these two limits from LEP when performing a general scan over the parameter space in Sec. VI; we expect strong constraints on the new charged VLLs lighter than 104 GeV.

C. LHC constraints on $E^\pm$ mass

After imposing the relic density constraint, we will see that all the points allowed at the electroweak scale receive an important contribution from coannihilation channels and therefore predict a small mass splitting Δ_m between the charged lepton and DM—see Fig. 6, which shows the variation of the relic density vs the DM mass. For a DM below the electroweak scale, a small mass splitting with the new charged $E^\pm$ is required to satisfy the relic density condition, which implies that it can easily be produced at colliders. Thus, constraints on the mass of the charged $E^\pm$ from searches for long-lived charged particles at the LHC [43–45] will strongly impact the possibility of having DM below the TeV scale. We used SModelS [46] as

TABLE I. Couplings relevant for annihilation and coannihilation processes (with $s_i^2 = 1 - c_i^2$ for $i = 1, 2$).

Vertex	Coupling expression	Vertex	Coupling expression
$N\bar{N}Z$	$\frac{ig_V}{8s_W}(c_2^4 s_1 s_2 \epsilon_2 - 2(c_2^2 s_2^3 + c_1^2 s_2^5)s_1^3\epsilon_1)\gamma^\mu + \frac{ig'}{8s_W}(c_2^3 s_2^3 \epsilon_2 - 2c_2 s_1^4 s_2^4 \epsilon_1)\gamma^\mu$	$\bar{N}E^-W^-$ NE^+W^+	$\frac{ig_V}{\sqrt{2}}\frac{c_W}{s_W} c_2 s_1 c_\beta s_\beta \epsilon_2 \gamma^\mu$
$N\bar{N}Z'$	$\frac{ig_V}{2} c_2 s_1 \gamma^\mu + \frac{ig'}{2} s_2 \gamma^\mu$	$\bar{N}E^-W'^-$ $NE^+W'^+$	$\frac{ig_V}{\sqrt{2}} s_1 \gamma^\mu$
$N\bar{N}Z''$	$\frac{ig_V}{2} c_1 \gamma^\mu$	$\bar{N}E^-W''^-$ $NE^+W''^+$	$\frac{ig_V}{\sqrt{2}} c_1 \gamma^\mu$
$E^+E^-\gamma$	$-i\, g\, s_W\, \gamma^\mu$	E^+E^-Z'	$-\frac{ig_V}{2} c_2 s_1 \gamma^\mu + \frac{ig'}{2} s_2 \gamma^\mu$
E^+E^-Z	$\frac{ig_V}{8s_W}(-c_2^4 s_1 s_2 \epsilon_2 + 2(c_2^2 s_2^3 + c_1^2 s_2^5)s_1^3\epsilon_1)\gamma^\mu + \frac{ig'}{8s_W}(c_2^3 s_2^3 \epsilon_2 - 2c_2 s_1^4 s_2^4 \epsilon_1 + 4c_2 s_W^2)\gamma^\mu$	E^+E^-Z''	$-\frac{ig_V}{2} c_1 \gamma^\mu$

TABLE II. Lower mass limits on $W'^{\pm}$, Z', $W''^{\pm}$, and Z'' for different benchmark values of g_V, based on Compact Muon Solenoid (CMS) data on W' production and decay via the $N_2\mu$ channel [40]. The condition $u_R = v_R + 100$ GeV is satisfied.

g_V	$m_{W'}$ [TeV]	$m_{Z'}$ [TeV]	$m_{W''}$ [TeV]	$m_{Z''}$ [TeV]
g	3.0	6.5	6.8	7.4
1	3.4	6.3	7.8	8.1
2	3.7	6.4	12.7	12.8
3	3.8	6.4	18.2	18.3

implemented in MICROMEGAs [47] to apply the LHC constraints on VLLs. We found that only a few points with a DM mass below the TeV scale evade the LHC constraints; in all cases, the DM mass is around 130 GeV. Note, however, that as we will see in Sec. VI, these same points will be excluded by DM direct detection.

V. DM OBSERVABLES: FIXED GAUGE BOSON MASSES

In this section, we calculate some DM observables for fixed gauge boson masses. We recall that the FeynRules package [48] is used to generate the model in CALCHEP [49] format. Throughout this article, we use micrOMEGAs [47] to calculate DM observables.

A. Relic density

The relic density Ωh^2 of N provides one of the most important experimental constraints on the model. We impose the condition that the total relic density falls within the observed range determined by the Planck Collaboration [22],

$$\Omega h^2 = 0.1184 \pm 0.0012. \tag{15}$$

We allow for a theoretical uncertainty of order 10% ($\Omega h^2 = [0.11, 0.13]$) as estimated in several studies [50–52]. Fixing the gauge boson masses at their lower limit as listed in Table II, we display in Fig. 2 the predicted value of Ωh^2 as a function of the DM mass for different choices of the coupling g_V. We can see from the different panels that DM is generally overabundant unless the mass of the DM lies around half of one of the vector boson mass. We choose two scenarios: the first features a large mass splitting between the DM and its charged partner $E^{\pm}$, $\Delta_m = 1$ TeV. For this case, the dominant channels are the annihilation ones mediated by the neutral gauge bosons. We notice that the relic density drops sharply when the mass of the DM becomes near $m_{Z'}/2$ and $m_{Z''}/2$. However, the strongly suppressed coupling of two DM to the Z boson does not allow it to attain $\Omega h^2 \approx 0.12$ when the DM mass is $m_Z/2$. In the second scenario, we take the mass splitting to be $\Delta_m = 1$ GeV. Thus, coannihilation effects becomes notable around half of the charged gauge

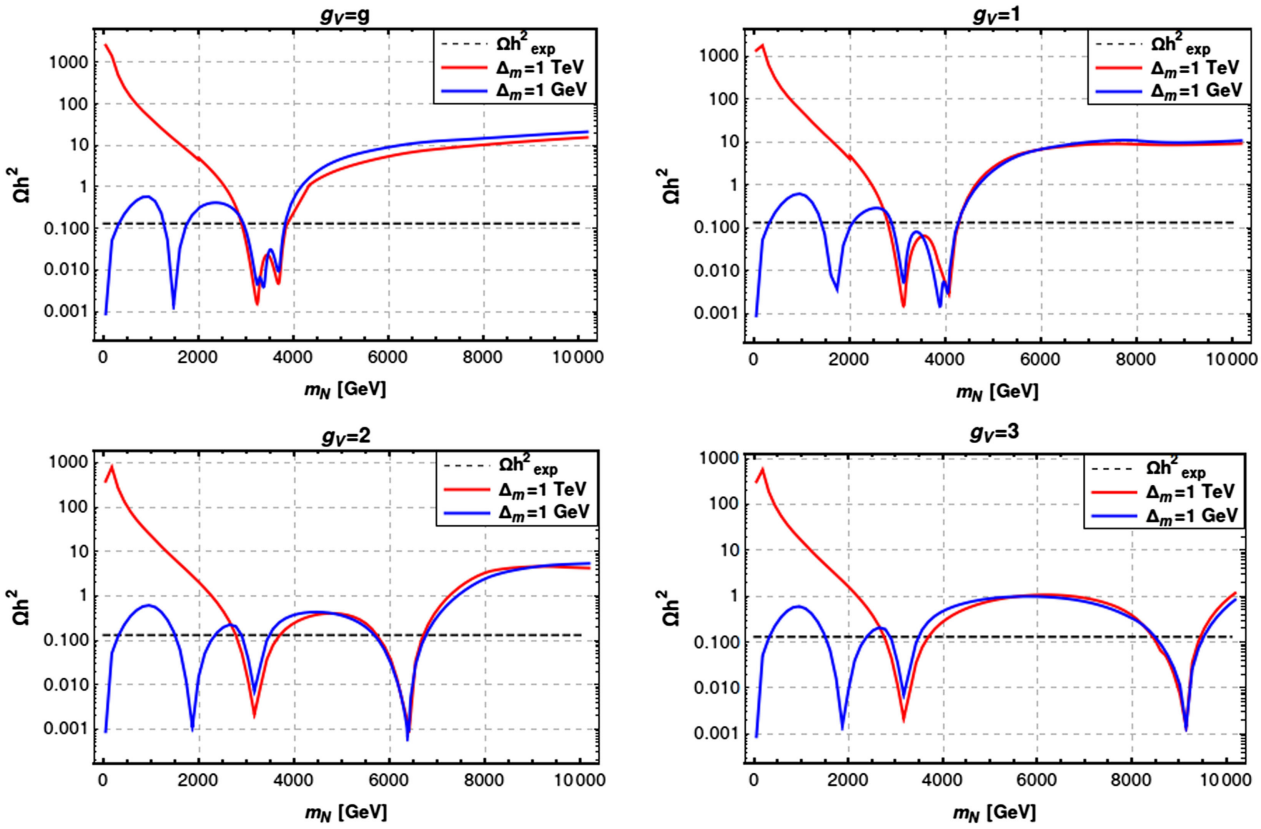

FIG. 2. Ωh^2 variation with respect to m_N for several benchmark values of the gauge coupling g_V.

bosons masses (see the blue lines in Fig. 2). The interaction of the DM particles and their charged partners via $W^{\pm}$ is suppressed as shown in Table I, but still leads to a correct value of Ωh^2 at the threshold of the process.

B. Direct detection

As mentioned above, the symmetry that enforces the Yukawa couplings of the VLLs-leptons to be zero with the aim of stabilizing the DM particle, entails that the DM candidate can interact with nucleons exclusively through the t-channel diagrams mediated by the neutral gauge bosons as shown in Fig. 3. For the same reason, there is no interaction of the DM with any scalar particles. Moreover, the structure of the model, where the VLLs belong to another gauge group $SU(2)_V$ and the bidoublet Φ—from which the Higgs particle originates—is chargeless under this group, entails that there is no interaction via the ordinary Higgs.

DM interacts with nucleons through spin-independent (SI) interactions, and the elastic scattering cross sections differ for neutrons (σ^n_{SI}) and protons (σ^p_{SI}). The behavior of the cross sections is determined by the relative contribution of the Z, Z', and Z'' exchange and of their interference. The Z, Z' exchange diagram leads to a much larger cross section for neutrons than protons while the Z'' exchange gives similar contributions. The value of the gauge coupling g_V has a significant impact on both cross sections, as can be seen in the left panel of Fig. 4. At small values of g_V, the Z' exchange dominates and destructive interference with the Z contribution suppresses σ^n_{SI} such that σ^p_{SI} is larger than σ^n_{SI}. As g_V increases, σ^p_{SI} decreases rapidly, mainly because the Z' contribution decreases; thus for $g_V \approx 0.7$, one gets an identical cross section for protons and neutrons. For larger values of g_V, the contribution of Z' to σ^n_{SI} becomes dominant and it increases steadily with g_V while the Z/Z'' exchange gives the subdominant contribution. For σ^p_{SI}, the behavior is quite different; for $g_V \approx 0.8$, there is a strong suppression of the Z contribution, while for $g_V \approx 1.6$, it is the Z' contribution that is strongly suppressed. Taking into account all interference effects, the minimum of the cross section is found around $g_V = 2.4$; for larger values of the coupling, all three gauge bosons contribute, nevertheless σ^p_{SI} is 2 orders of magnitude smaller than σ^n_{SI}. These results were obtained for $m_N = 2$ TeV; note, however, that the same feature occurs for other DM masses as the SI cross sections are basically independent of m_N, as can be seen in the right panel of Fig. 4.

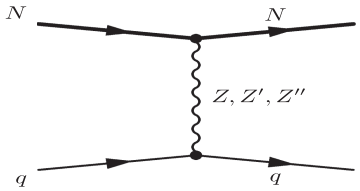

FIG. 3. Feynman diagrams for the DM elastic scattering off nucleons.

Since the neutrons or protons contributions are not necessarily equal, measuring the nuclear recoil energy from the elastic scattering off nucleus would provide appropriate constraints on parameter space of the model in comparing the results from the DD experiments. The current most restricted limits are coming from the LZ experiment [23] and the future projections from XLZD [26]. Thus, computing the normalized to one nucleon cross section for a pointlike xenon nucleus would be more convenient in aim to directly compare with the experimental limits [53],

$$\sigma^{Xe}_{SI} = \frac{4\mu_N^2}{\pi}\frac{(Zf_p + (A-Z)f_n)^2}{A^2}, \tag{16}$$

where $\mu_N = \frac{m_N m_n}{m_N + m_n}$ is the reduced mass of the DM with the nucleon (n), Z ($A - Z$) is the number of protons (neutrons) in the xenon nucleus, and $f_{p,n}$ are the couplings to protons and neutrons.

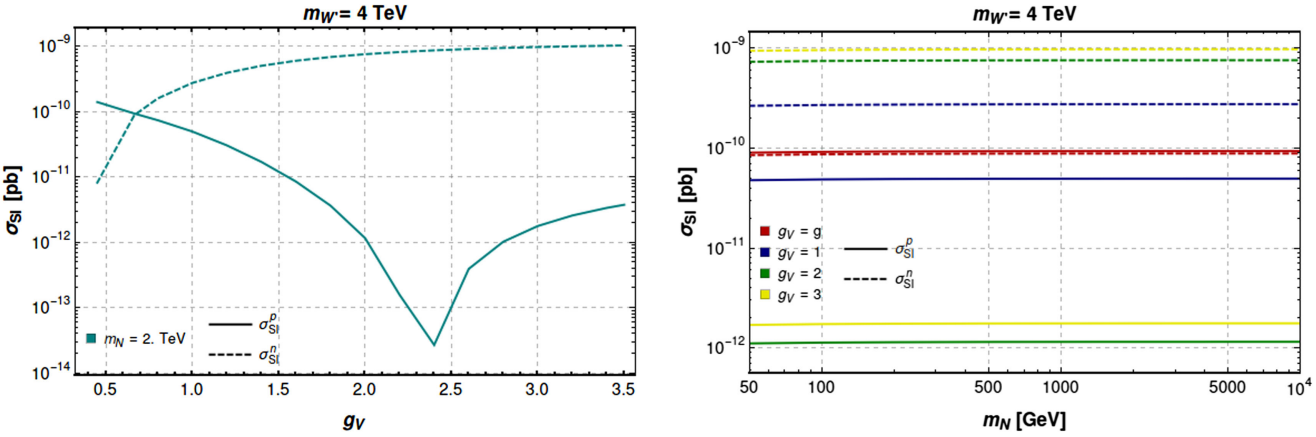

FIG. 4. Left: σ_{SI} off proton and neutron variation with respect to g_V for a benchmark value of $m_N = m_{W'}/2 = 2$ TeV. Right: σ_{SI} off proton and neutron variation with respect to m_N for a benchmark value of $m_{W'} = 4$ TeV and several values of g_V.

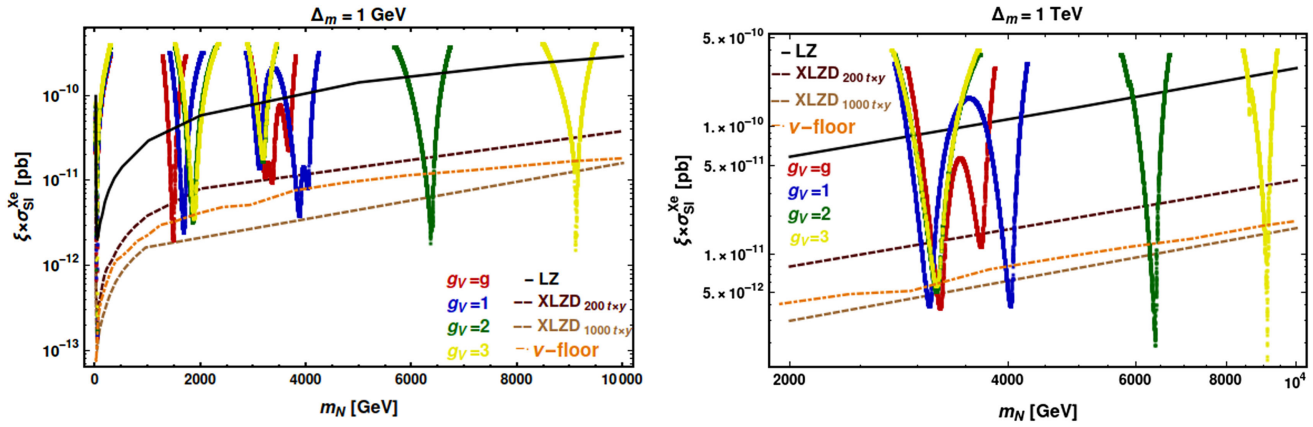

FIG. 5. $\xi \times \sigma_{SI}^{Xe}$ with respect to m_N for two scenarios of mass splitting $\Delta_m = 1$ GeV (TeV) and several benchmark values of g_V. The thick black line represents the current limits of LZ experiment [23], the brown dashed lines represent the future projection limits of XLZD for exposures $200t \times y$ and $1000t \times y$ [26], and the orange dash-dotted line represents the neutrino floor [54].

We fixed first the gauge bosons masses at their lower limits as provided in Table II and fixed the masses of the HNs to be half of $m_{W'}$ for each benchmark value of g_V. Then, using micrOMEGAs, we made a random scan over m_N where we imposed that the relic density constraints should be satisfied, whether our candidate explains all the DM in the Universe or part of it. The results are shown in Fig. 5, where we plot the rescaled SI cross section off xenon $\xi \times \sigma_{SI}^{Xe}$ with respect to m_N, where ξ is the fraction of the predicted value of the relic density over the observed value. Because of the contributions from both the annihilation and coannihilation processes to the relic density, the $\Delta_m = 1$ GeV scenario (left panel) drops sharply when m_N is around half of the neutral and charged gauge bosons masses. The valid points at the GeV scale appear since the relic density condition is satisfied because of the coannihilation channels contribution that are mediated by the $W^{\pm}$ boson, and disappear as expected regarding the other scenario when $\Delta_m = 1$ TeV (right panel) where the relic density condition is not satisfied (see Fig. 2).

The plots indicate that only the region near a gauge boson resonance is allowed by current LZ limits, and that most of these regions are within the reach of the future XLZD projections. Note, however, that some of the points cannot be probed since they fall below the neutrino floor [54]. In Fig. 5, the neutral gauge bosons masses were fixed at their lower bounds, and we expect that the SI scattering cross section will decrease for heavier masses (see Fig. 8), thus allowing a wider range of allowed points. In the next section, we will explore the full parameter space of the model. In this general scan, we will also apply collider constraints, namely the LEP 1 [41] and LEP 2 [42] limits, in addition to the LHC searches for long-lived charged particles [43–45] embedded in `SModelS` [46]. As a result, the viable points at the electroweak scale will be strongly suppressed. Moreover, we will show that the TeV scale DM can be constrained from indirect searches, in particular from the limits on DM annihilation into photons from CTA [27].

VI. GENERAL SCAN

The four free parameters for our study have been discussed in Sec. II. The gauge coupling g_V is fixed to four benchmarks values; see Table III. The remaining three parameters are varied randomly, taking into consideration the collider constraints on the gauge bosons masses from Table II. The range considered is represented in Table III.

A. Relic density

For this general scan, we impose only an upper bound on the value of the relic density, $\Omega h^2 < 0.13$. This value includes a 10% theoretical uncertainty as in Sec. V A. As discussed in the previous section, DM (co-)annihilation is most efficient when the gauge boson exchanged in s-channel is near resonance. Since the masses of the new gauge bosons are above 3 TeV, the upper bound on the relic density requires in general a dark matter mass above 1.5 TeV. Figure 6 shows the predicted value of the relic density as a function of the DM mass for two different values of the gauge coupling g_V. The mass splitting Δ_m is indicated by the color palette. Figure 6 also shows that a few points are found for a DM mass below 200 GeV; these are associated with a very small mass splitting between the dark matter and the charged VLL and correspond to coannihilation channels

TABLE III. The range of the four free parameters used in the scan.

g_V	$m_{W'}$
g	3–10 TeV
1	3.4–10 TeV
2	3.7–10 TeV
3	3.8–10 TeV
m_N	10 GeV–10 TeV
Δ_m	1 MeV–1 TeV

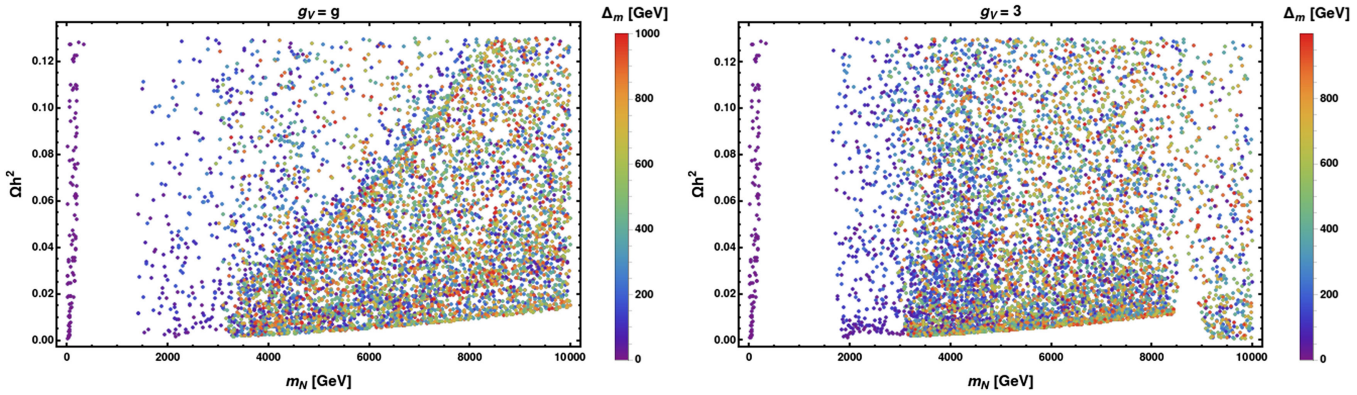

FIG. 6. Ωh^2 variation with respect to m_N for two benchmark values of the gauge coupling g_V, with the color palette indicating the splitting mass Δ_m.

mediated by $W^{\pm}$ exchange. Note that at this point, we have not imposed the collider constraints on charged leptons mentioned in Sec. IV. Such constraints will exclude most of the low mass region as will be discussed next.

B. Direct detection and collider searches

Before examining the predictions for DM direct detection, we apply the LEP and LHC constraints on the charged partner, $E^{\pm}$. For a DM at the electroweak scale, the relic density imposes a very small mass splitting which implies a new charged lepton that can easily be produced at colliders. Thus, nearly all the points at the electroweak scale are excluded. More specifically, all points in the region $m_E < m_Z/2$ are excluded by the LEP 1 constraint on the Z boson partial width, while those with $m_E < 104$ GeV are excluded by the LEP 2 search for charginos. For masses around 130 GeV, a few points are compatible with the LHC searches for long-lived charged particles embedded in `SModelS`. However, all of these points are excluded by the direct detection limits from LZ [23]. This can be seen in Fig. 7, which shows the prediction for the rescaled SI cross section $\xi \times \sigma_{SI}^{Xe}$ with respect to m_N for four benchmark values of g_V, together with the current best limit from LZ [23]. Figure 7 also shows that for DM masses above 1.5 TeV, a fraction of the points is already excluded by the LZ limits; moreover, another large fraction is within the reach of future experiments such as XLZD [26]. We also note that an important fraction of the points lies below the neutrino floor. However, we will see in the next section that some will be within reach of future indirect searches.

The main contribution for the elastic scattering cross section of dark matter on nucleons comes mainly from diagrams with Z' or Z'', since these contributions go as $1/m_{Z'}^4$ or $1/m_{Z''}^4$ respectively. The largest cross sections, and thus the points excluded by LZ in Fig. 7, are found for the smallest allowed values of the gauge boson masses, as shown in Fig. 8. This figure shows the variation of $\xi \times \sigma_{SI}^{Xe}$ with respect to the extra neutral gauge boson masses, where the black points represent the ones excluded by LZ. As expected, the largest cross sections correspond to the lighter gauge boson masses. It also illustrates that for large values of g_V (right panel when $g_V = 3$), the mass splitting between Z' and Z'' increases in comparison with low values of g_V (left panel when $g_V = g$). Thus, one can distinguish the regions where Z' or Z'' give the dominant contribution in Fig. 7. Moreover this large mass splitting entails that for large values of g_V it can become difficult to satisfy the relic density constraint because only one generation of gauge bosons contributes in DM annihilation processes, hence the empty area in the lower panels of Fig. 7 around $m_N \approx 8$–9 TeV.

C. Indirect detection bounds

DM can be detected indirectly by observing γ rays originating from its annihilation in galaxies. As mentioned in Sec. III, the annihilation process could proceed either through an s-channel mediated by the vector bosons portal or through t-channels mediated by the VLLs themselves [see Fig. 1 and Eq. (13)]. As discussed before, the interaction with the Z boson is highly suppressed and can be ignored. For a TeV scale dark matter mass, the dominant annihilation channels are into quarks, leptons, and pairs of HNs. These processes proceed via Z'/Z'' exchange in the s-channel. Other possible final states include pairs of neutrinos, HNs with ν_i, pairs of neutral or charged gauge bosons, or even Z/Z' with h. However, all these final states are subdominant.

The photon spectra originating from all final states are computed with micrOMEGAs and these spectra are compared with the one from dwarf spheroidal galaxies observed by Fermi-LAT [24,25] with the function embedded within micrOMEGAs [47]. We find that these data do not allow us to constrain the model further, as expected for TeV scale DM. Here, we have not included the points at lower DM masses which are already excluded by DD and collider searches.

A better probe of TeV scale DM is expected in the future with the CTA telescope. To determine the potential of CTA to probe the model, we again use micrOMEGAs to compare the total photon spectra corresponding to each scenario

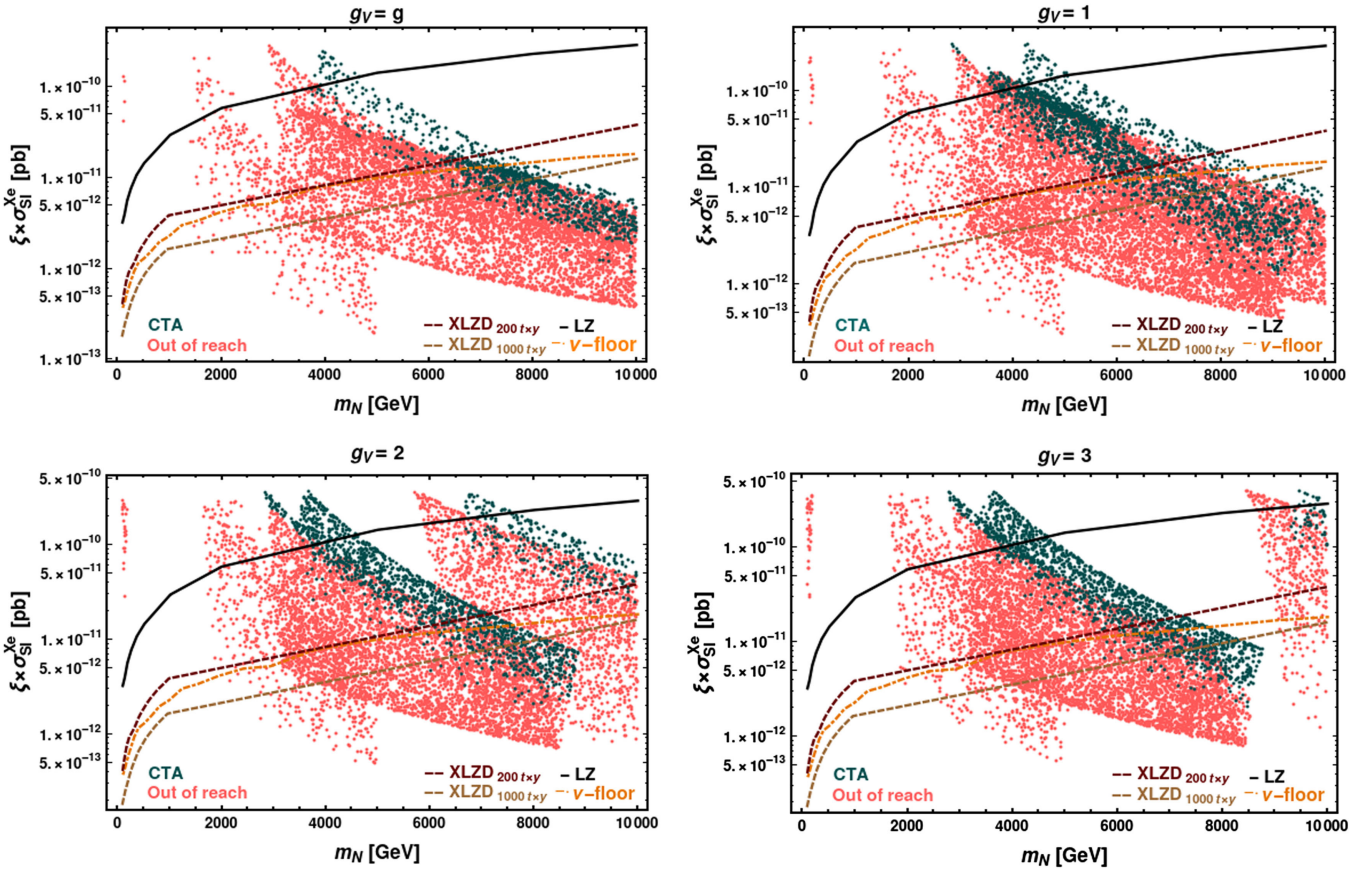

FIG. 7. $\xi \times \sigma_{SI}^{Xe}$ with respect to m_N for $g_V = g, 1, 2, 3$. The thick black line represent the current LZ limit [23], the brown dashed lines represent the future projection limits of XLZD for exposures $200t \times y$ and $1000t \times y$ [26], and the orange dash-dotted line represents the neutrino floor [54]. The blue night color represent the cases where the points are within the reach of CTA [27].

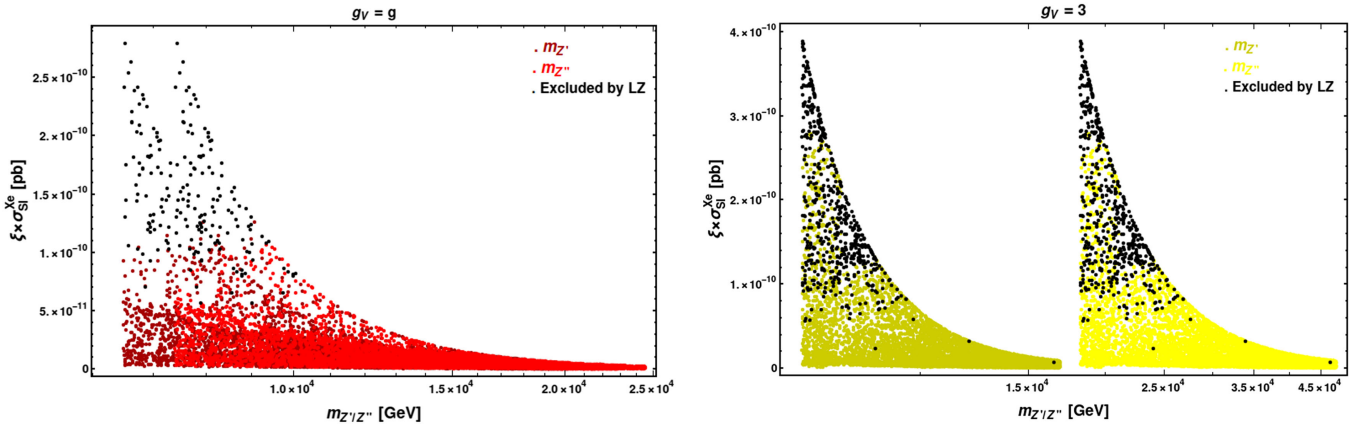

FIG. 8. $\xi \times \sigma_{SI}^{Xe}$ variation with respect to the extra neutral gauge boson masses for two benchmark values of the gauge coupling $g_V = g, 3$.

with the projections of CTA [27]. Figure 9 shows the predictions for the rescaled cross section annihilation $\langle \sigma_V \rangle$ (i.e., $\xi^2 \times \langle \sigma_V \rangle$) as a function of m_N for the four benchmark values of g_V. With the factor ξ^2, the cases where DM is under abundant is taken into account.

In Fig. 9, the spread of viable points in the range $m_N \sim$ 1.5–5 TeV features a very suppressed value of $\xi^2 \times \langle \sigma_V \rangle$. These points correspond to coannihilation scenarios with s-channel exchange of $W'^{\pm}$ and a small mass splitting between the component of the VLL doublet. For these

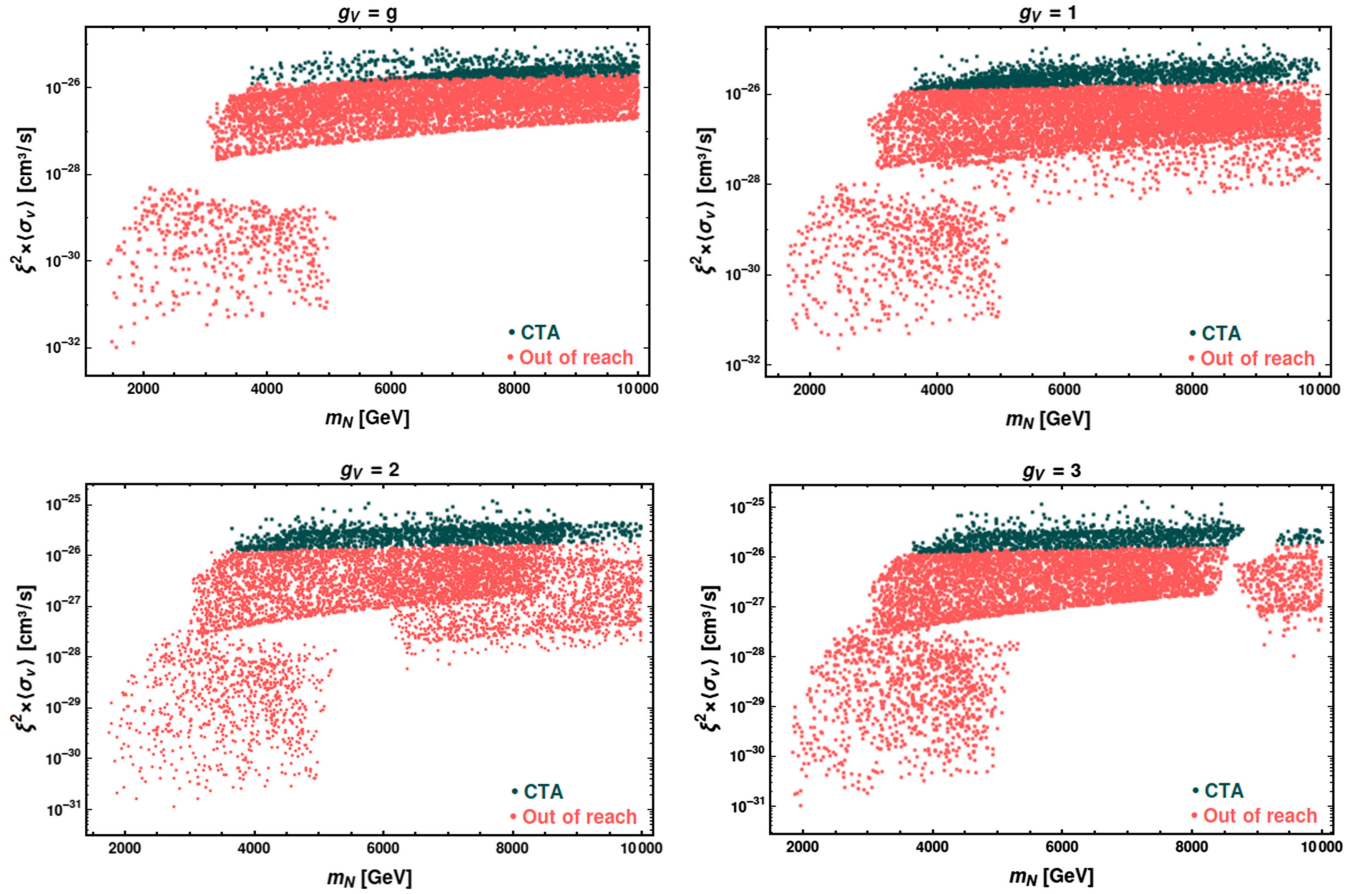

FIG. 9. $\xi^2 \times \langle \sigma_V \rangle$ with respect to m_N for several benchmark values of the gauge coupling g_V. The blue night color represent scenarios within reach of CTA. The light red points satisfy collider constraints and are beyond the reach of DD.

points, not only can the relic density be small ($\xi \ll 1$), but also the cross section for pair annihilation of DM can be much suppressed as it does not set the relic density. For the bulk of the points at the TeV scale, the predictions for $\xi^2 \times \langle \sigma_V \rangle$ lie in the range 10^{-28}–10^{-25} cm^3/s, thus points in the upper range fall within the reach of CTA. Note that in this region, the relic density is mainly determined by gauge boson exchange, either a combination of Z'/Z'', or $W'^{\pm}, W''^{\pm}$ bosons in case of coannihilation. For DM pair annihilation mediated through the s-channel exchange of Z'/Z'', the dominant final states are $q\bar{q}$, l^+l^- and N_iN_i. We conclude that a significant fraction of those points are within the reach of CTA. The range of masses for Z'/Z'' is illustrated in Fig. 10, and one clearly sees that points with large $\xi^2 \times \langle \sigma_V \rangle$ within the reach of CTA are close to the region $2m_N \approx m_{Z'}$ or $m_{Z''}$. Moreover, the distinct region with suppressed $\xi^2 \times \langle \sigma_V \rangle$ in Fig. 9 which does not respect this mass relation can be clearly identified with both cases of Fig. 10.

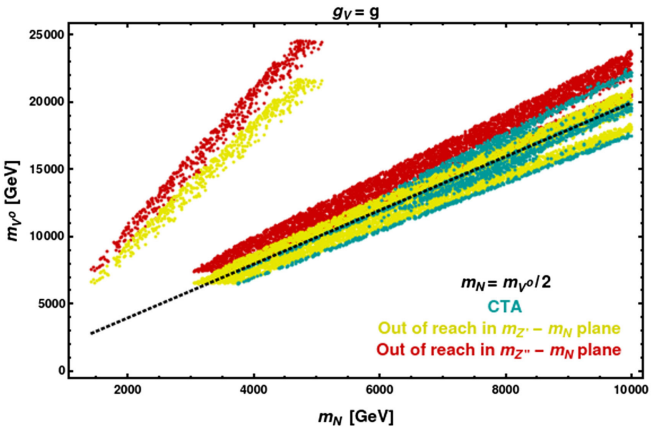

FIG. 10. Masses of neutral gauge bosons with respect to m_N mass for $g_V = g$. The cyan points are within reach of CTA while the red and yellow points are out of reach of DD and ID. All points satisfy collider constraints. The dotted line represents $m_N = m_{Z'}/2, m_{Z''}/2$.

VII. CONCLUSION

In this work, we have shown that an extension of the LRSM with an extra $SU(2)_V$ factor and one generation of VLLs can provide a good DM candidate, the neutral component of the VLL doublet. For stabilizing the DM particle, a discrete parity symmetry that forbids the mixing of VLLs-leptons has been imposed, thus the dark sector

particles interact only with vector bosons. DM annihilation and coannihilation into fermions proceed mainly through exchange of the vector bosons portal in s-channel, otherwise annihilation into final state bosons proceed through VLLs exchange in t-channel.

After imposing an upper bound on the relic density, we found that DM could be either at the electroweak scale or at the (multi) TeV scale. For the low mass region, a small mass splitting between the DM particle and its charged partner is required. However, searches for charged leptons at LEP and LHC almost completely exclude this possibility. The only remaining points above 104 GeV are found to be incompatible with direct detection results of LZ. For DM above the TeV scale, all viable points escape the current limits from dwarf spheroidal galaxies by Fermi-LAT; however, the model is partly constrained by direct detection results of LZ and will be further probed by future large detectors. Moreover, we have highlighted a complementarity between DD and ID. In particular, the future CTA telescope will be able to probe multi-TeV DM that escape multiton scale direct detectors such as XLZD, and even to probe some points that fall below the neutrino floor.

In this work, we have made simplifying assumptions; for one, we only considered the case where the mass of the HNs is half that of $m_{W'}$ in order to adapt simply the existing LHC limits on new gauge bosons coming from the $W'^{\pm} \to N_2\mu^{\pm}$ channel. We found that the contribution of final states with pair of HNs give a non-negligible contribution to DM annihilation, although the annihilation into quarks and leptons remain dominant. We checked that removing the HNs from the final state did not affect significantly the photon spectra. We conclude that allowing a larger mass range for the HNs is more likely to impact the DM observables only if it impacts the allowed masses for the new gauge bosons.

Finally, in our analysis all the masses of extra scalars were fixed at a high scale, an open question that we leave for future work is whether taking the scalar sector particles into consideration—where neutral, charged, and doubly charged scalars could appear in the final states of annihilation and coannihilation processes—would impact DM observables.

DATA AVAILABILITY

The data are not publicly available. The data are available from the authors upon reasonable request.

[1] J. C. Pati and A. Salam, Lepton number as the fourth color, Phys. Rev. D **10**, 275 (1974); **11**, 703(E) (1975).

[2] R. N. Mohapatra and J. C. Pati, A natural left-right symmetry, Phys. Rev. D **11**, 2558 (1975).

[3] G. Senjanovic and R. N. Mohapatra, Exact left-right symmetry and spontaneous violation of parity, Phys. Rev. D **12**, 1502 (1975).

[4] P. Duka, J. Gluza, and M. Zralek, Quantization and renormalization of the manifest left-right symmetric model of electroweak interactions, Ann. Phys. (N.Y.) **280**, 336 (2000).

[5] A. Roitgrund, G. Eilam, and S. Bar-Shalom, Implementation of the left-right symmetric model in FeynRules, Comput. Phys. Commun. **203**, 18 (2016).

[6] N. G. Deshpande, J. F. Gunion, B. Kayser, and F. I. Olness, Left-right symmetric electroweak models with triplet Higgs, Phys. Rev. D **44**, 837 (1991).

[7] R. N. Mohapatra, *Unification and Supersymmetry: The Frontiers of Quark-Lepton Physics*, 3rd ed. (Springer, New York, 2022).

[8] R. N. Mohapatra, Mechanism for understanding small neutrino mass in superstring theories, Phys. Rev. Lett. **56**, 561 (1986).

[9] R. N. Mohapatra and J. W. F. Valle, Neutrino mass and baryon number nonconservation in superstring models, Phys. Rev. D **34**, 1642 (1986).

[10] M. Nemevsek, G. Senjanovic, and Y. Zhang, Warm dark matter in low scale left-right theory, J. Cosmol. Astropart. Phys. 07 (2012) 006.

[11] J. Heeck and S. Patra, Minimal left-right symmetric dark matter, Phys. Rev. Lett. **115**, 121804 (2015).

[12] W.-l. Guo, L.-m. Wang, Y.-l. Wu, and C. Zhuang, The dark matter constraints on the left-right symmetric model with Z_2 symmetry, Phys. Rev. D **78**, 035015 (2008).

[13] W.-L. Guo, L.-M. Wang, Y.-L. Wu, Y.-F. Zhou, and C. Zhuang, Gauge-singlet dark matter in a left-right symmetric model with spontaneous *CP* violation, Phys. Rev. D **79**, 055015 (2009).

[14] S. Patra and S. Rao, Singlet fermion dark matter within left-right model, Phys. Lett. B **759**, 454 (2016).

[15] C. Garcia-Cely and J. Heeck, Phenomenology of left-right symmetric dark matter, J. Cosmol. Astropart. Phys. 03 (2016) 021.

[16] S. Bhattacharyya and A. Datta, Dark matter perspective of left-right symmetric gauge model, Nucl. Phys. B **991**, 116197 (2023).

[17] A. Berlin, P. J. Fox, D. Hooper, and G. Mohlabeng, Mixed dark matter in left-right symmetric models, J. Cosmol. Astropart. Phys. 06 (2016) 016.

[18] P. S. B. Dev, R. N. Mohapatra, and Y. Zhang, Heavy right-handed neutrino dark matter in left–right models, Mod. Phys. Lett. A **32**, 1740007 (2017).

[19] S. Bahrami, M. Frank, D. K. Ghosh, N. Ghosh, and I. Saha, Dark matter and collider studies in the left-right symmetric model with vectorlike leptons, Phys. Rev. D **95**, 095024 (2017).

[20] Y. Bouzeraib and M. S. Zidi, Alternative framework for the left-right symmetric model including vector-like fermions, arXiv:2603.07608.
[21] G. Belanger, A. Pukhov, and G. Servant, Dirac neutrino dark matter, J. Cosmol. Astropart. Phys. 01 (2008) 009.
[22] N. Aghanim *et al.* (Planck Collaboration), Planck 2018 results. VI. Cosmological parameters, Astron. Astrophys. **641**, A6 (2020); **652**, C4(E) (2021).
[23] J. Aalbers *et al.* (LZ Collaboration), Dark matter search results from 4.2 tonne-years of exposure of the LUX-ZEPLIN (LZ) experiment, Phys. Rev. Lett. **135**, 011802 (2025).
[24] V. Bonnivard *et al.*, Dark matter annihilation and decay in dwarf spheroidal galaxies: The classical and ultrafaint dSphs, Mon. Not. R. Astron. Soc. **453**, 849 (2015).
[25] A. Alvarez, F. Calore, A. Genina, J. Read, P. D. Serpico, and B. Zaldivar, Dark matter constraints from dwarf galaxies with data-driven J-factors, J. Cosmol. Astropart. Phys. 09 (2020) 004.
[26] J. Aalbers *et al.*, A next-generation liquid xenon observatory for dark matter and neutrino physics, J. Phys. G **50**, 013001 (2023).
[27] A. Acharyya *et al.* (CTA Collaboration), Sensitivity of the Cherenkov telescope array to a dark matter signal from the Galactic centre, J. Cosmol. Astropart. Phys. 01 (2021) 057.
[28] Y. Zhang, H. An, X. Ji, and R. N. Mohapatra, Right-handed quark mixings in minimal left-right symmetric model with general CP violation, Phys. Rev. D **76**, 091301 (2007).
[29] L. Lopez Honorez, E. Nezri, J. F. Oliver, and M. H. G. Tytgat, The inert doublet model: An archetype for dark matter, J. Cosmol. Astropart. Phys. 02 (2007) 028.
[30] L. Lopez Honorez and C. E. Yaguna, The inert doublet model of dark matter revisited, J. High Energy Phys. 09 (2010) 046.
[31] L. Lopez Honorez and C. E. Yaguna, A new viable region of the inert doublet model, J. Cosmol. Astropart. Phys. 01 (2011) 002.
[32] B. Batell, Dark discrete gauge symmetries, Phys. Rev. D **83**, 035006 (2011).
[33] M. Hirsch, S. Morisi, E. Peinado, and J. W. F. Valle, Discrete dark matter, Phys. Rev. D **82**, 116003 (2010).
[34] L. Lavoura, S. Morisi, and J. W. F. Valle, Accidental stability of dark matter, J. High Energy Phys. 02 (2013) 118.
[35] K. Earl, K. Hartling, H. E. Logan, and T. Pilkington, Two viable large scalar multiplet models with a Z_2 symmetry, Phys. Rev. D **90**, 055029 (2014); **92**, 039902(E) (2015).
[36] E. Ma and A. Natale, Scotogenic Z_2 or $U(1)_D$ model of neutrino mass with $\Delta(27)$ symmetry, Phys. Lett. B **734**, 403 (2014).
[37] S. Baek, P. Ko, and W.-I. Park, Local Z_2 scalar dark matter model confronting galactic GeV-scale γ-ray, Phys. Lett. B **747**, 255 (2015).
[38] J. M. Lamprea and E. Peinado, Seesaw scale discrete dark matter and two-zero texture Majorana neutrino mass matrices, Phys. Rev. D **94**, 055007 (2016).
[39] G. Bélanger, S. Choubey, R. M. Godbole, S. Khan, M. Mitra, and A. Roy, WIMP and FIMP dark matter in singlet-triplet fermionic model, J. High Energy Phys. 11 (2022) 133.
[40] A. Tumasyan *et al.* (CMS Collaboration), Search for a right-handed W boson and a heavy neutrino in proton-proton collisions at $\sqrt{s} = 13$ TeV, J. High Energy Phys. 04 (2022) 047.
[41] D. Abbaneo *et al.* (ALEPH, DELPHI, L3, OPAL, LEP Electroweak Working Group, SLD Heavy Flavor, and Electroweak Groups Collaborations), A combination of preliminary electroweak measurements and constraints on the standard model, arXiv:hep-ex/0112021.
[42] A. Heister *et al.* (ALEPH Collaboration), Search for charginos nearly mass degenerate with the lightest neutralino in e^+e^- collisions at center-of-mass energies up to 209-GeV, Phys. Lett. B **533**, 223 (2002).
[43] M. Aaboud *et al.* (ATLAS Collaboration), Search for heavy charged long-lived particles in the ATLAS detector in 36.1 fb^{-1} of proton-proton collision data at $\sqrt{s} = 13$ TeV, Phys. Rev. D **99**, 092007 (2019).
[44] S. Chatrchyan *et al.* (CMS Collaboration), Searches for long-lived charged particles in pp collisions at $\sqrt{s} = 7$ and 8 TeV, J. High Energy Phys. 07 (2013) 122; 11 (2022) 149 (E).
[45] V. Khachatryan *et al.* (CMS Collaboration), Constraints on the pMSSM, AMSB model and on other models from the search for long-lived charged particles in proton-proton collisions at $\sqrt{s} = 8$ TeV, Eur. Phys. J. C **75**, 325 (2015).
[46] M. M. Altakach, S. Kraml, A. Lessa, S. Narasimha, T. Pascal, C. Ramos, Y. Villamizar, and W. Waltenberger, SModelS v3: Going beyond $\mathcal{Z}_2$ topologies, J. High Energy Phys. 11 (2024) 074.
[47] G. Alguero, G. Belanger, F. Boudjema, S. Chakraborti, A. Goudelis, S. Kraml, A. Mjallal, and A. Pukhov, micrOMEGAs 6.0: N-component dark matter, Comput. Phys. Commun. **299**, 109133 (2024).
[48] A. Alloul, N. D. Christensen, C. Degrande, C. Duhr, and B. Fuks, FeynRules 2.0—A complete toolbox for tree-level phenomenology, Comput. Phys. Commun. **185**, 2250 (2014).
[49] A. Belyaev, N. D. Christensen, and A. Pukhov, CalcHEP 3.4 for collider physics within and beyond the Standard Model, Comput. Phys. Commun. **184**, 1729 (2013).
[50] S. Banerjee, F. Boudjema, N. Chakrabarty, G. Chalons, and H. Sun, Relic density of dark matter in the inert doublet model beyond leading order: The heavy mass case, Phys. Rev. D **100**, 095024 (2019).
[51] S. Banerjee, F. Boudjema, N. Chakrabarty, and H. Sun, Relic density of dark matter in the inert doublet model beyond leading order for the low mass region: I. Renormalisation and constraints, Phys. Rev. D **104**, 075002 (2021).
[52] G. Bélanger, A. Pukhov, C. E. Yaguna, and Ó. Zapata, The Z_7 model of three-component scalar dark matter, J. High Energy Phys. 03 (2023) 100.
[53] G. Belanger, J. Da Silva, and A. Pukhov, The right-handed sneutrino as thermal dark matter in U(1) extensions of the MSSM, J. Cosmol. Astropart. Phys. 12 (2011) 014.
[54] J. Billard, L. Strigari, and E. Figueroa-Feliciano, Implication of neutrino backgrounds on the reach of next generation dark matter direct detection experiments, Phys. Rev. D **89**, 023524 (2014).